First-principles investigation of magnetocrystalline anisotropy at the L 2 1 full Heusler | MgO interfaces and tunnel junctions

Rajasekarakumar Vadapoo, Ali Hallal, Hongxin Yang, Mairbek Chshiev

First-principles investigation of magnetocrystalline anisotropy at the $L2_1$ full Heusler|MgO interfaces and tunnel junctions

Rajasekarakumar Vadapoo,[1,2,3,*] Ali Hallal,[1,2,3] Hongxin Yang,[1,2,3] and Mairbek Chshiev[1,2,3]
[1]*Univ. Grenoble Alpes, INAC-SPINTEC, F-38000 Grenoble, France*
[2]*CNRS, SPINTEC, F-38000 Grenoble, France*
[3]*CEA, INAC-SPINTEC, F-38000 Grenoble, France*
(Received 8 June 2016; published 16 September 2016)

Magnetocrystalline anisotropy at Heusler alloy|MgO interfaces has been studied using first-principles calculations. It has been found that Co-terminated Co_2FeAl|MgO interfaces show perpendicular magnetic anisotropy up to 1.31 mJ/m^2, while those with FeAl termination exhibit in-plane magnetic anisotropy. Atomic layer-resolved analysis indicates that the origin of perpendicular magnetic anisotropy in Co_2FeAl|MgO interfaces can be attributed to the out-of-plane orbital contributions of interfacial Co atoms. At the same time, Co_2MnGe and Co_2MnSi interfaced with MgO tend to favor in-plane magnetic anisotropy for all terminations.

DOI: 10.1103/PhysRevB.94.104418

I. INTRODUCTION

Perpendicular magnetic anisotropy (PMA) in transition metal|insulator interfaces has been demonstrated more than a decade ago [1,2]. These interfaces have become a viable alternative to PMA in fully metallic structures based on heavy nonmagnetic elements with strong spin-orbit coupling (SOC) [3–6]. Indeed, high PMA values have been observed in Co(Fe)|MOx (M = Ta, Mg, Al, Ru, etc.) interfaces despite their weak SOC [1,2]. These structures serve as the main constituents for perpendicular magnetic tunnel junctions (p-MTJs) which are very promising for realizing the next generation of high-density nonvolatile memories and logic devices [7–11]. One of the most important requirements for the use of p-MTJs in spintronic applications including high-density spin transfer torque magnetic random access memory (STT-MRAM) is a combination of large PMA, high thermal stability, and low critical current to switch magnetization of the free layer. A CoFeB|MgO p-MTJ is one of the most promising candidates among state-of-the-art structures [10]. However, another class of ferromagnetic electrode materials with drastically improved characteristics for use in p-MTJs is Heusler alloys, since they possess much higher spin polarization [12] and significantly lower Gilbert damping [13].

Full Heusler alloy (X_2YZ)|MgO interfaces with high interfacial PMA and weak SOC have been gaining interest recently [12,14–16]. For instance, MgO-based MTJs with Co_2FeAl (CFA) electrodes show high PMA in most of the experiments. The surface anisotropy energy (K_s) is found to be around 1 mJ/m^2 for Pt|CFA|MgO trilayers [17] and CFA|MgO [16,18] interfaces. The observed PMA values for these structures are comparable to those reported for CoFeB|MgO [10] and tetragonally distorted $Mn_{2.5}Ga$ films grown on Cr-buffered MgO [14]. However, there are reports on observation of in-plane magnetic anisotropy (IMA) for CFA|MgO interfacial structures in different cases [19,20]. Thus, these interfaces show PMA with values between 0.16 and 1.04 mJ/m^2 [16,21,22] as well as IMA with K_s = −1.8 mJ/m^2 [19]. On the other hand, some theoretical studies have reported a PMA value of 1.28 mJ/m^2 for Co-terminated structures [23] and an IMA value of 0.78 mJ/m^2 [23] and a PMA value of 0.428 mJ/m^2 [24] for FeAl-terminated structures. It has been suggested that interfacial Fe atoms are responsible for PMA in these structures [21] but the microscopic origins of anisotropy remain to be clarified further.

In order to elucidate the origin of PMA in these interfaces, we present a systematic study of magnetic anisotropy in Heusler alloy (X_2YZ)|MgO interfaces [with X = Co, YZ = FeAl, MnGe and MnSi] using the first-principles method. We explore the different interfacial conditions in these interfaces. In order to understand the microscopic mechanism of PMA, we employ the on-site projected and orbital-resolved analysis of magnetocrystalline anisotropy energy (MAE) which allows identification of atomic layer contributions along with the corresponding different orbital contributions [25,26]. We found that the magnetic anisotropy is much more complex compared to that in Co(Fe)|MgO structures [26] and it is strongly dependent on the interface termination and composition.

II. METHODS

Calculations were performed using the Vienna *ab initio* siumulation package (VASP) [27,28] with generalized gradient approximation [29] and projected augmented wave potentials [30,31]. We used the kinetic energy cutoff of 600 eV and a Monkhorst-Pack K-point grid of 13 × 13 × 3 where the convergence of MAE is checked with repect to the number of K-points. Initially the structures were relaxed in volume and shape until the force acting on each atom fell below 1 meV/Å. The Kohn-Sham equations were then solved to find the charge distribution of the ground state system without taking spin-orbit interactions (SOI) into account. Finally, the total energy of the system was calculated for a given orientation of magnetic moments in the presence of spin-orbit coupling using a non-self-consistent calculation. The surface magnetic anisotropy energy K_s is calculated as $(E^{\parallel} - E^{\perp})/a^2$, where a is the in-plane lattice constant and $E^{\perp}$ ($E^{\parallel}$) represents the energy for the out-of-plane [001] (in-plane

*Present address: Geophysical Laboratory, Carnegie Institution of Washington, Washington, D.C. 20015, USA.

[100]) magnetization orientation with respect to the interface. The in-plane anisotropy (the difference between [100] and [110]) has been checked and found to be negligible. Positive and negative values of K_s correspond to out-of-plane and in-plane anisotropy, respectively. In addition, we define the effective anisotropy $K_{\text{eff}} = K_s/t_{\text{CFA}} - E_{\text{demag}}$, where E_{demag} is the demagnetization energy which is the sum of all the magnetostatic dipole-dipole interactions up to infinity. We adopt the dipole-dipole interaction method to calculate the E_{demag} term instead of $2\pi M_s^2$, where M_s is the saturation magnetization, since the latter underestimates this term for thin films. [26,32,33] In VASP the spin-orbit term is evaluated using the second-order approximation:

$$H_{\text{SOC}} = \frac{1}{2(m_e C)^2}\frac{1}{r}\frac{dV}{dr}\vec{L}\cdot\vec{s}, \tag{1}$$

where V denotes the spherical part of all-electron Kohn-Sham potentials inside the PAW spheres, and $\vec{L}$ and $\vec{s}$ represent the angular momentum operator and the Pauli spin matrices, respectively. The spin-orbit coupling then can be calculated for each orbital angular momentum, from which one can extract atomic layer- and orbital-resolved MAE [26,33–35].

III. RESULTS

Full-Heusler (X_2YZ) alloys are intermetallic compounds with a cubic $L2_1$ structure and belong to the space group $Fm\bar{3}m$ [12,36]. The Heusler|MgO interfaces have been setup with the crystallographic orientation of Heusler(001)[100] ‖ MgO(001)[110] [24,37–39]. This results in a relatively low lattice mismatch between Heusler(001) and MgO(001) with a 45° in-plane rotation. The energetically stable X and YZ terminations at the interface were studied and are denoted as X-Heusler|MgO and YZ-Heusler|MgO as shown, respectively, in Figs. 1(a) and 1(b). The results of these interfaces are compared to those of the X-Heusler|vacuum and YZ-Heusler|vacuum slabs shown in Figs. 1(c) and 1(d), respectively.

Increasing the MgO thickness beyond 5 atomic layers (i.e. monolayers denoted further ML) is found to have no effect on magnetic anisotropy. The variation of surface magnetic anisotropic energy (K_s) with the thickness t of Heusler layers varying from 3 to 11 ML for the Heusler|MgO interfaces is shown in Fig. 2. One can see that only the Co-CFA|MgO structure gives rise to very high PMA which weakly depends on CFA thickness, while the FeAl-CFA|MgO and all CMG|MgO as well as CMS|MgO show IMA. It is interesting to note that the magnetic anisotropy energies for CMG|MgO and CMS|MgO as a function of thickness follow similar trends which might be due to the inert nature of the Z element (Ge, Si). The in-plane anisotropy contribution in these structures increases as a function of thickness and stabilizes after 9 ML. It can be seen that K_s for Co-CFA|MgO increases from 1.20 mJ/m^2 to a maximum of 1.31 mJ/m^2 at 7 ML thickness (∼0.8 nm), which is in agreement with the experimental findings of Gabor *et al.* [22] and Wen *et al.* [16]. The inset in Fig. 2 shows the corresponding effective anisotropy ($K_{\text{eff}} * t$) as a function of CFA thickness. It shows a decaying behavior and vanishes around 11 ML becoming IMA beyond this thickness, in reasonable agreement with recent experiments [16,22].

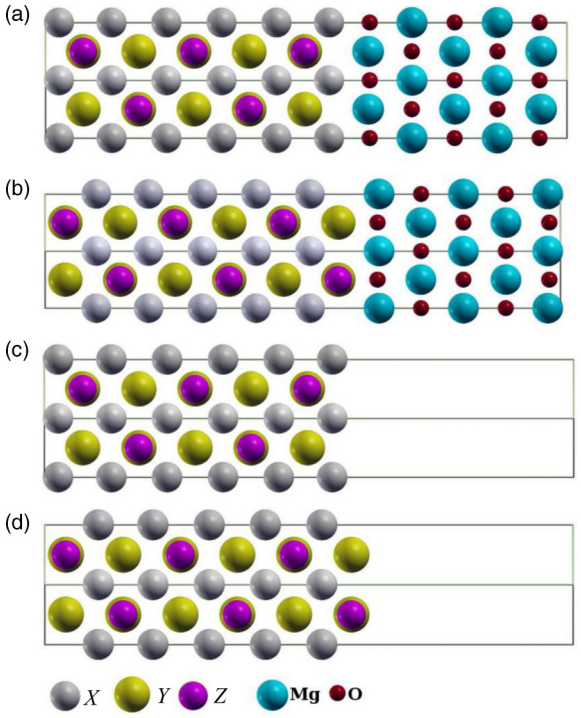

FIG. 1. Perspective view of (a) X-terminated and (b) YZ-terminated interface structures of Heusler (X_2YZ)|MgO and of (c) X-terminated and (d) YZ-terminated Heusler|Vacuum slabs with X = Co and YZ = FeAl, MnGe, and MnSi. Grey, yellow, pink, blue, and red spheres represent X, Y, Z, Mg, and O atoms, respectively.

In order to understand the origin of PMA and the effect of MgO, we examined the on-site projected magnetic anisotropy for the 11 ML of Heusler|MgO and their free surface counterparts as shown in Fig. 3. As one can see, the

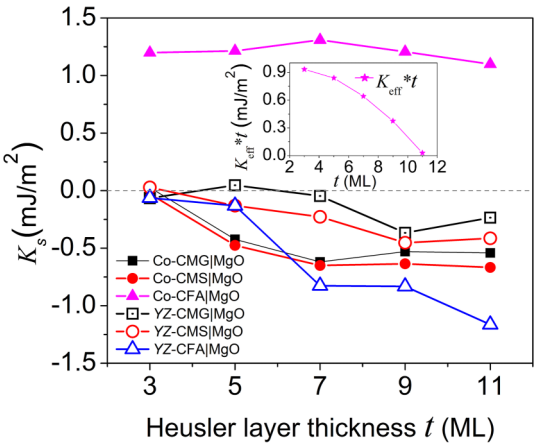

FIG. 2. Surface magnetic anisotropy energy (K_s) as a function of the number of Heusler atomic layers (ML) in Co and YZ-terminated Heusler (X_2YZ)|MgO structures. Filled data points represent Co-terminated interfaces and open data points represent YZ-terminated interfaces. Magenta triangles represent Co_2FeAl (CFA) interfaces, black squares represent Co_2MnGe (CMG) interfaces, and red circles represent Co_2MnSi (CMS) interfaces. Inset shows the effective anisotropy ($K_{\text{eff}} * t$) as a function of the thickness of CFA in the Co-terminated CFA|MgO interface.

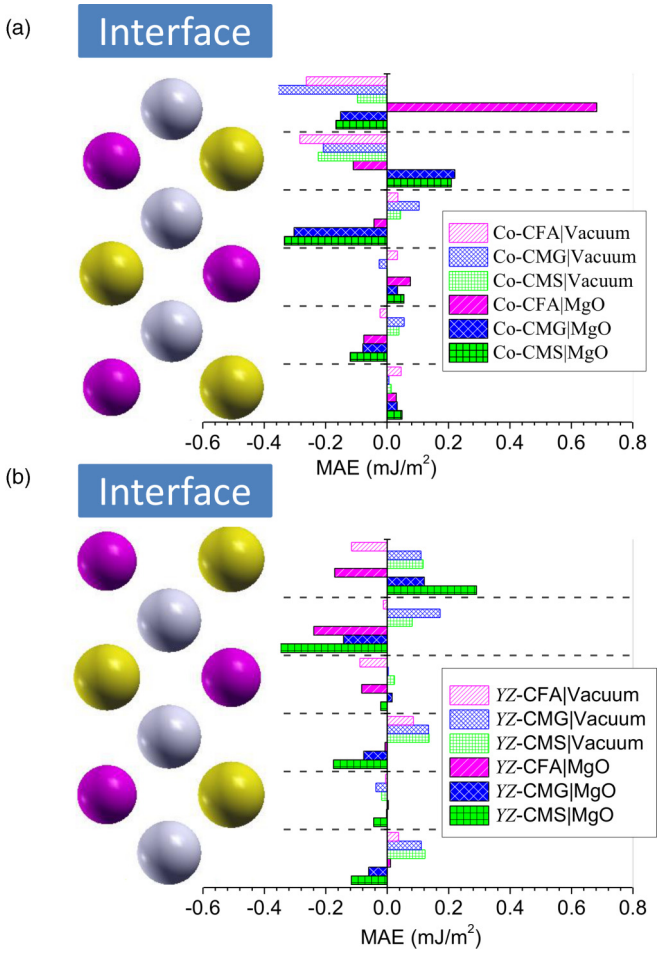

FIG. 3. Atomic layer-resolved contributions to the anisotropy for (a) X-terminated and (b) YZ-terminated Heusler|MgO (solid filled bars) and Heusler|vacuum (light filled bars) structures shown in Figs. 1(a) and 1(c) and Figs. 1(b) and 1(d), respectively. The Co_2FeAl (CFA), Co_2MnGe (CMG), and Co_2MnSi (CMS) cases are represented by pink, blue, and green bars, respectively. The side views of the corresponding Heusler layers are shown on the left for convenience.

major PMA contribution of 0.69 mJ/m^2 in the Co-CFA|MgO structure comes from the interfacial Co atoms while the inner atomic layers show a fair amount of in-plane or out-of-plane contributions represented by solid pink bars in Fig. 3(a). By comparing with the CFA|vacuum structure shown by unfilled pink bars in the same figure, we can clearly identify that the presence of MgO on top of the Co layer plays a decisive role in establishing the PMA in the Co-terminated CFA|MgO structure. More complicated behavior is observed for Co-CMG and Co-CMS structures where the role of MgO in anisotropy varies depending on the atomic layer. While it tends to decrease (increase) the IMA in the first Co layer for Co-CMG (Co-CMS), it simultaneously flips the IMA into PMA (PMA into IMA) for the second YZ (third Co) layer.

A similar nontrivial picture is observed for YZ-terminated structures shown in Fig. 3(b). By employing the same analysis in order to clarify the role of MgO vs vacuum next to the YZ-terminated Heusler alloy, one can see that the MgO has a tendency to improve the IMA for the case of YZ-CFA for all

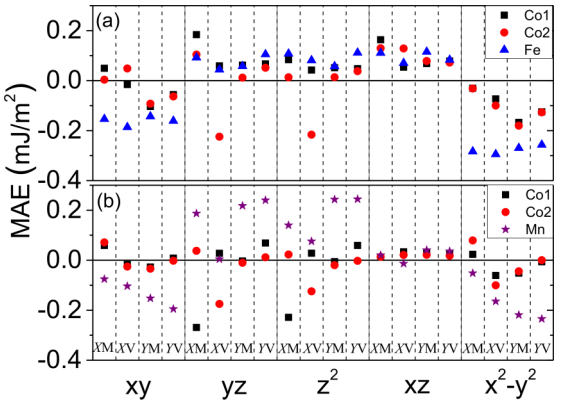

FIG. 4. d-orbital-resolved contributions to magnetic anisotropy for interfacial atoms in X- and YZ-terminated (a) $Co_2FeAl|MgO$ and (b) $Co_2MnGe|MgO$ structures along with their free surface counterparts. Black squares, red circles, blue triangles, and purple stars represent contributions from orbitals with d-character of two Co (Co1 and Co2 within the same atomic layer), Fe, and Mn atoms, respectively. XV, XM, YV and YM denote X-Heusler|vacuum, X-Heusler|MgO, YZ-Heusler|vacuum and YZ-Heusler|MgO interfaces respectively.

layers. Furthermore, it enhances the PMA (IMA) for the first (all Co) layers of YZ-CMS and YZ-CMG structures.

Overall it can be concluded that the presence of MgO tends to favor IMA from all Co layers except the interfacial ones in Co-CFA and Co-CMG structures. At the same time, the inner YZ layers in the presence of MgO have a tendency for the PMA for Co-terminated structures]Fig. 3(a)], while the YZ interfacial layer favors the IMA (PMA) in YZ-CFA (YZ-CMS and YZ-CMG) [cf. Fig. 3(b)].

To further elucidate the microscopic origin of PMA, we carried out the d-orbital-resolved magnetic anisotropy contributions for interfacial atoms as shown in Fig. 4. One can see that the switch from IMA to PMA when MgO is placed on top of Co-terminated CFA mainly arises from the out-of-plane orbitals ($d_{xz,yz}$ and d_{z^2}) as shown by comparison of the XV and XM columns in Fig. 4(a). Furthermore, this switch is assisted by all d orbitals within the second (YZ) layer. At the same time, the MgO-induced enhancement of the IMA in the first two layers from the interface (FeAl and Co) in the case of YZ-terminated CFA [see Fig. 3(b)] is due to a increase (decrease) of the IMA (PMA) contribution from $d_{x^2-y^2}$ (d_{yz} and d_{z^2}) orbitals, as seen from comparison of columns YV and YM in Fig. 4(a).

In the case of Co-terminated CMG, the effect of MgO results in an overall tendency to decrease the IMA with participation of in-plane d orbitals (d_{xy} and $d_{x^2-y^2}$) in the first Co layer with quite interesting opposite contributions from out-of-plane d_{yz} and d_{z^2} orbitals [see XV and XM columns in Fig. 4(b)]. At the same time, for the second layer (MnGe) contribution, the presence of MgO has a clear tendency to switch from IMA into PMA assisted by all d orbitals. As for Mn-terminated CMG, the presence of MgO has almost no effect on the first MnGe layer anisotropy contributions, while it induces the flip from PMA to IMA from almost all d orbitals within the second Co layer [Fig. 4(b)]. The orbital

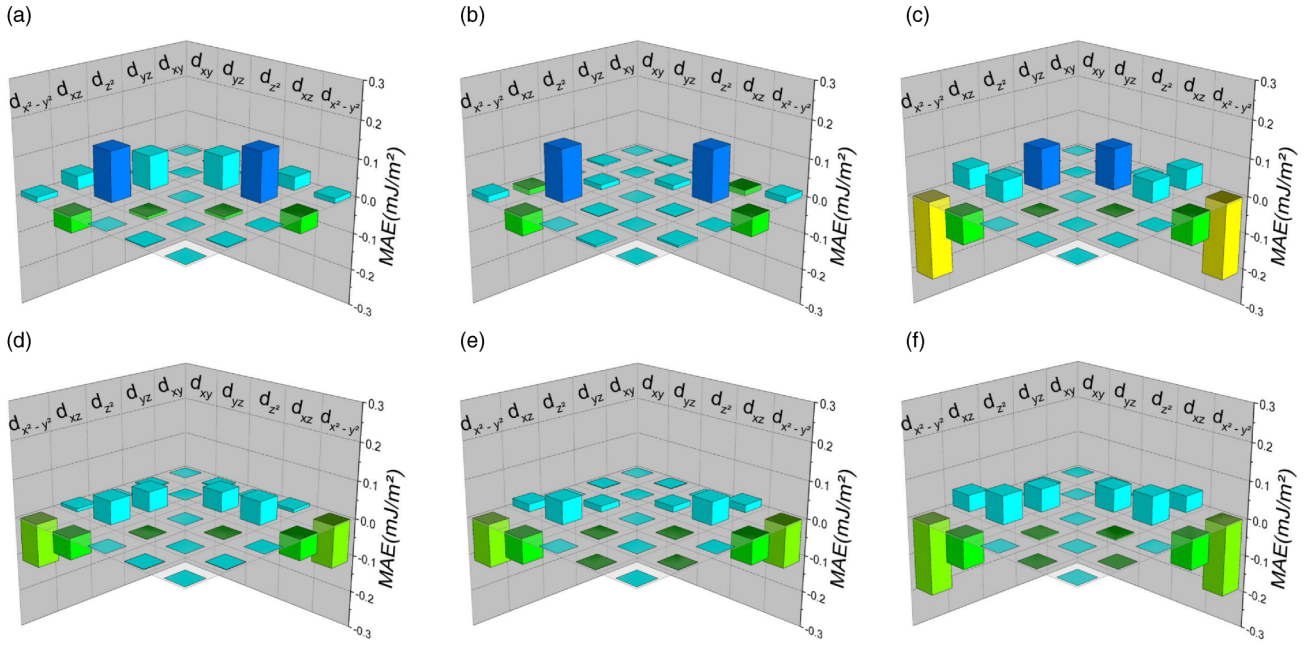

FIG. 5. Magnetic anisotropy contribution from different d-orbital hybridizations at the interfacial atoms of (a) [(d)] Co1, (b) [(e)] Co2, and (c) [(f)] Fe for the Co-terminated $Co_2FeAl|MgO$ interface [FeAl-terminated interface].

contributions for CMS are found to be very similar to CMG orbital contributions.

To further elucidate the PMA origin in $Co_2FeAl|MgO$, Fig. 5 shows the magnetic anisotropy contribution originated from the SOC-induced hybridizations between different orbital channels for interfacial atoms at the Co-terminated and FeAl-terminated interfaces. In all cases the out-of-plane orbitals' ($d_{xz(yz)}$, d_{z^2}) mutual hybridizations strongly favor PMA contributions. At the same time, hybridization among in-plane orbitals (d_{xy}, $d_{x^2-y^2}$) gives rise to IMA except for the case of Co1 and Co2 atoms in the Co-terminated interface where they have a slight PMA contribution. In all cases, $d_{x^2-y^2}$ hybridization with out-of-plane, mainly d_{yz}, orbitals contributes to IMA. On the other hand, d_{xy} hybridization with out-of-plane, mainly d_{xz}, orbitals contributes to PMA except for the case of the Co2 atom in the Co-terminated structure. However, the sum of the contributions coming from Co1 and Co2 atoms favors PMA.

IV. DISCUSSION

Aforementioned analysis shows that the Co-CFA|MgO structure favors the high PMA while YZ termination in the CFA|MgO structure gives rise to IMA. This allows us to conclude that interfacial Co atoms are responsible for PMA. However, it has been claimed recently that the origin of PMA could be attributed to Fe atoms at the interface in CFA|MgO [21] using X-ray magnetic circular dichroism (XMCD) measurements in combination with Bruno's model analysis [40]. In order to resolve this disagreement, we carried out the orbital momentum calculations for a 7-ML structure corresponding to that reported in experiments [21] with both terminations. We systematically found that per atomic layer resolved orbital moment anisotropy is inconsistent with atomic layer-resolved MAE contributions for Co layers while it remains in qualitative agreement for layers containing Fe. We can therefore conclude that Bruno's model should be used with caution and its validity may depend on a particular system.

In summary, using first-principles calculations we investigated the magnetic anisotropy of Full Heusler|MgO interfaces and MTJs for all terminations. It was found that Co-terminated CFA|MgO shows a PMA value of 1.31 mJ/m^2 induced by the presence of MgO in agreement with recent experiments while FeAl-terminated CFA and other structures possess IMA. We also unveiled the microscopic mechanisms of PMA in Heusler|MgO structures by evaluating the on-site projected and orbital-resolved contributions to magnetic anisotropy and found that interfacial Co atoms are responsible for high PMA (IMA) in CFA (CMG, CMS). Finally, out-of-plane (in-plane) orbitals tend to favor mainly PMA (IMA).

ACKNOWLEDGMENTS

The authors thank C. Tiusan for fruitful discussions. This work was supported by EU M-ERA.NET HeuMem and ANR SPINHALL, and SOSPIN projects.

[1] S. Monso *et al.*, Appl. Phys. Lett. **80**, 4157 (2002).
[2] B. Rodmacq, S. Auffret, B. Dieny, S. Monso, and P. Boyer, J. Appl. Phys. **93**, 7513 (2003).
[3] N. Nakajima, T. Koide, T. Shidara, H. Miyauchi, H. Fukutani, A. Fujimori, K. Iio, T. Katayama, M. Nývlt, and Y. Suzuki, Phys. Rev. Lett. **81**, 5229 (1998).

[4] P. F. Carcia, A. D. Meinhaldt, and A. Suna, Appl. Phys. Lett. **47**, 178 (1985).
[5] H. J. G. Draaisma, W. J. M. de Jonge, and F. J. A. den Broeder, J. Magn. Magn. Mater. **66**, 351 (1987).
[6] D. Weller, Y. Wu, J. Stöhr, M. G. Samant, B. D. Hermsmeier, and C. Chappert, Phys. Rev. B **49**, 12888 (1994).
[7] G. Kim *et al.*, Appl. Phys. Lett. **92**, 172502 (2008).
[8] L. E. Nistor, B. Rodmacq, S. Auffret, and B. Dieny, Appl. Phys. Lett. **94**, 012512 (2009).
[9] L. E. Nistor, B. Rodmacq, S. Auffret, A. Schuhl, M. Chshiev, and B. Dieny, Phys. Rev. B **81**, 220407 (2010).
[10] S. Ikeda *et al.*, Nat. Mater. **9**, 721 (2010).
[11] M. Endo, S. Kanai, S. Ikeda, F. Matsukura, and H. Ohno, Appl. Phys. Lett. **96**, 212503 (2010).
[12] T. Graf, C. Felser, and S. S. S. Parkin, Prog. Solid State Chem. **39**, 1 (2011).
[13] C. Liu, C. K. A. Mewes, M. Chshiev, T. Mewes, and W. H. Butler, Appl. Phys. Lett. **95**, 022509 (2009).
[14] F. Wu *et al.*, Appl. Phys. Lett. **94**, 122503 (2009).
[15] W. Wang, H. Sukegawa, and K. Inomata, Appl. Phys. Express **3**, 093002 (2010).
[16] Z. Wen, H. Sukegawa, S. Mitani, and K. Inomata, Appl. Phys. Lett. **98**, 242507 (2011).
[17] X. Li *et al.*, Appl. Phys. Express **4**, 043006 (2011).
[18] Y. Cui *et al.*, Appl. Phys. Lett. **102**, 162403 (2013).
[19] M. Belmeguenai, H. Tuzcuoglu, M. S. Gabor, T. Petrisor, Jr., C. Tiusan, D. Berling, F. Zighem, T. Chauveau, S. M. Chérif, and P. Moch, Phys. Rev. B **87**, 184431 (2013).
[20] M. Belmeguenai *et al.*, J. Magn. Magn. Mater. **399**, 199 (2016).
[21] J. Okabayashi, H. Sukegawa, Z. Wen, K. Inomata, and S. Mitani, Appl. Phys. Lett. **103**, 102402 (2013).
[22] M. S. Gabor, T. Petrisor, and C. Tiusan, J. Appl. Phys. **114**, 063905 (2013).
[23] M. Tsujikawa, D. Mori, Y. Miura, and M. Shirai, in *Proceedings of MML 2013—8th International Symposium on Metallic Multilayers, Mo-8, Kyoto Research Park, Kyoto, Japan, May 19–24*, 2013.
[24] Z. Bai *et al.*, New J. Phys. **16**, 103033 (2014).
[25] H. X. Yang, M. Chshiev, B. Dieny, J. H. Lee, A. Manchon, and K. H. Shin, Phys. Rev. B **84**, 054401 (2011).
[26] A. Hallal, H. X. Yang, B. Dieny, and M. Chshiev, Phys. Rev. B **88**, 184423 (2013).
[27] G. Kresse and J. Hafner, Phys. Rev. B **47**, 558 (1993).
[28] G. Kresse and J. Furthmuller, Phys. Rev. B **54**, 11169 (1996).
[29] Y. Wang and J. P. Perdew, Phys. Rev. B **44**, 13298 (1991).
[30] G. Kresse and D. Joubert, Phys. Rev. B **59**, 1758 (1999).
[31] P. E. Blöchl, Phys. Rev. B **50**, 17953 (1994).
[32] G. H. O. Daalderop, P. J. Kelly, and M. F. H. Schuurmans, Phys. Rev. B **41**, 11919 (1990).
[33] A. Hallal, B. Dieny, and M. Chshiev, Phys. Rev. B **90**, 064422 (2014).
[34] S. Peng *et al.*, Sci. Rep. **5**, 18173 (2015).
[35] H. Yang *et al.*, Nano Lett. **16**, 145 (2015).
[36] C. A. Culbert, M. Williams, M. Chshiev, and W. H. Butler, J. Appl. Phys. **103**, 07D707 (2008).
[37] M. Yamamoto *et al.*, J. Phys. D: Appl. Phys. **39**, 824 (2006).
[38] M. S. Gabor, T. Petrisor, C. Tiusan, M. Hehn, and T. Petrisor, Phys. Rev. B **84**, 134413 (2011).
[39] X. Lu, K. L. Varaha, K. Mukherjee, and N. C. Kar, IEEE Trans. Magn. **49**, 3965 (2009).
[40] P. Bruno, Phys. Rev. B **39**, 865 (1989).